STUDY ON EVALUATION METHOD FOR TRANSIENT RESPONSE OF CONDUCTOR SURFACE TO LARGE PULSE CURRENT*

H. Iinuma†, H. Sato, Ibaraki University, Ibaraki, Japan
T. Takayanagi, Japan Atomic Energy Agency, Tōkai Mura, Japan
Y. Tanaka, Kyokuto Boeki Kaisha LTD, Tokyo, Japan

Abstract

To measure spin precession in ultra-precise magnetic fields, a method for three-dimensional spiral beam injection has been developed. For example, a muon beam with a momentum of 300 MeV/c must be confined within a controlled storage region (radius 33.3 ± 1.5 cm, height ± 5 cm) in a solenoid-type storage magnet (central magnetic flux density 3 T) based on medical MRI technology, with the local magnetic field variation controlled to be less than 0.1 ppm. A vertical kick by magnetic field is required to suppress the motion in the axial direction of the solenoid, and trial calculations have shown that a pulsed magnetic field can be excited by applying a pulsed current with a half-sine waveform (peak current 1 kA, pulse width 120 ns, frequency 25 Hz) to a kicker coil with a radius of 37 cm and a height of 10 cm. Generating a magnetic field using an extremely fast pulsed current requires a calculation method that takes into account the transient response on the conductor surface, with a skin effect of approximately 35 μm. In this presentation, we will apply the OPERA model to the geometry of the current kicker field generating conductor, and discuss the modeling by practicable mesh on the conductor surface and the evaluation of the time-space distribution of the generated kicker field. In addition, we will also discuss the model calculation method including the wall of the vacuum chamber around the kicker device.

INTRODUCTION

In this paper, we focus on the kicker system designed to control the longitudinal motion along the solenoid axis while maintaining a circular orbit with a radius of 0.33 m, and to confine the beam within the effective magnetic field region (weak focusing potential) of the solenoidal magnet. A key feature of the kicker system is that the conductor carrying the pulsed high current covers the entire storage orbit. By placing an axially symmetric kicker coil conductor inside an axially symmetric solenoidal magnetic field, an axisymmetric pulsed magnetic field is generated. This configuration ensures that the beam is naturally confined to an axisymmetric orbit, leading to highly stable beam motion during storage. The overall concept of the three-dimensional spiral injection is shown in Fig. 1 and described in Ref. [1]. Details of superconducting storage magnet design and field calculation method are given in Refs. [2] and [3].

* Work supported by JSPS KAKENHI Grant Nos. 26287055, 19H00673, 22K14061, and 23KJ0590.
† hiromi.iinuma.spin@vc.ibaraki.ac.jp

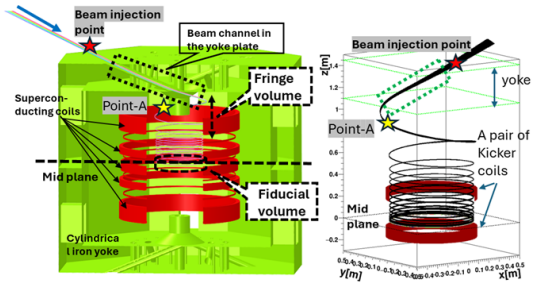

Figure 1: Schematic view of the solenoidal storage magnet and beam injection configuration.

BEAM DYNAMICS DURING THE KICK

Figure 2 shows the longitudinal motion of 1000 particles injected with optimized beam shaping and tracked under the kicker field. The trajectory is sampled every 10 ps (1000 slices correspond to 10 ns). After the kick, 974 particles are confined within $|z| < 0.05$ m, demonstrating efficient longitudinal confinement. Details of phase space matching, so-called a strong X-Y coupling, for the three-dimensional spiral injection is described in Ref. [4].

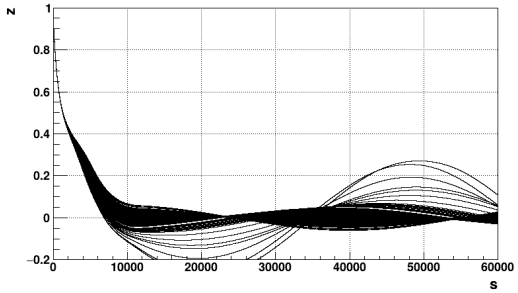

Figure 2: Longitudinal motion of 1000 particles during and after the kicker, showing confinement along the solenoid axis.

Vertical Phase Space

Figure 3 shows the longitudinal phase-space motion along the solenoid axis. The gray curves represent 200 trajectories, and the colored filamentary structures correspond to selected slices of 1000 trajectories. The kink structure around $0.2<z<0.5$ m originates from the focusing effect of the kicker field. Since the solenoidal field provides strong radial focusing but weak control in the longitudinal direction, the kicker field is required to suppress the beam spread during injection. This enables efficient capture of the beam into the weak focusing potential, defining the primary role of the kicker system.

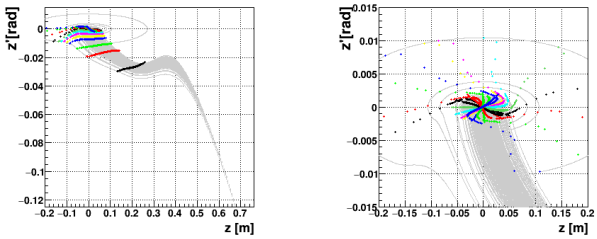

Figure 3: Longitudinal phase-space distribution illustrating the filamentary structure and focusing by the kicker.

Conservation of Eigen Emittance

The kicker induces a non-adiabatic perturbation, leading to a temporary deviation from symplectic transport. However, the eigen-emittances are not strictly conserved during the kick, indicating a transient mode transition. Figure 4 shows the evolution of the eigen-emittances and correlation coefficients during the kicker. At each slice, the covariance matrix is constructed from 1000 particles in the six-dimensional phase space, and the corresponding eigen-emittances are evaluated as a function of slice. The correlation components derived from the covariance matrix are also shown. As a result, the eigen-emittances are not strictly conserved during the kick, indicating a transient mode transition. After the kick, the beam motion becomes stable and the phase-space structure is reorganized. The calculation method for the covariance matrix and eigen-emittances is described in Ref. [5].

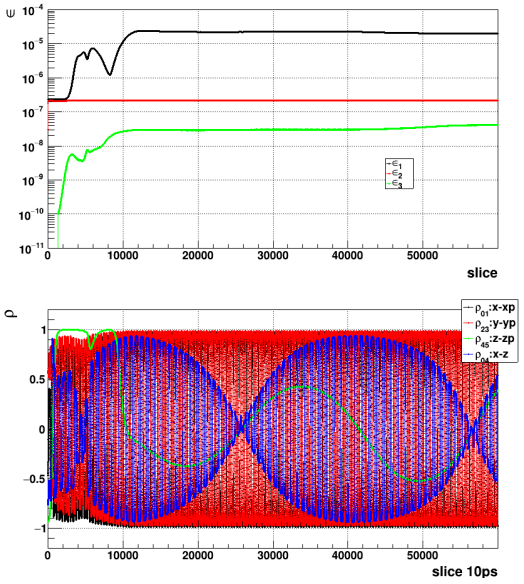

Figure 4: Evolution of eigen-emittances and correlation coefficients during the kicker.

Figure 5 shows enlarged views of the correlation coefficients ρ during the kicker and in the storage region. The rapid variation of ρ during the kick indicates a transient reorganization of the phase-space. In contrast, the regular oscillation observed in the storage region corresponds to a coherent rotation of the phase-space distribution. This is consistent with the filamentary structures in the time-slice representation, where the beam distribution forms a rotating "string-like" pattern.

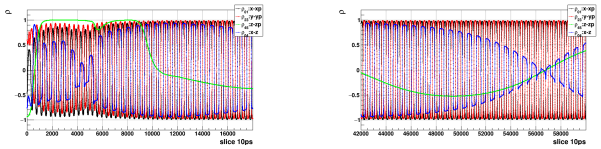

Figure 5: Enlarged views of correlation coefficients showing phase-space reorganization and coherent rotation.

Beam Transport Matrices and Symplecticity

Figure 6 shows $\|\Delta M\|$ and $\|\Delta C\|$ along the trajectory. While the eigen-emittances are approximately conserved, the transport is not strictly symplectic. Here, $\Delta M = M^T J M - J$ quantifies the deviation from symplecticity, and ΔC represents the affine contribution. Both quantities remain stable in the storage region, indicating stable beam dynamics. Details are given in Ref. [5].

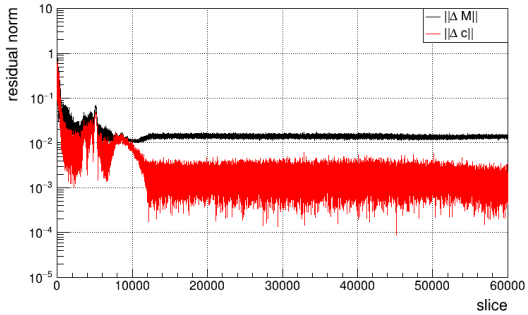

Figure 6: Residual norms of transport matrix and affine components indicating deviation from symplecticity.

These results show that, when the injection parameters are properly matched to the magnetic field configuration, an ideal phase-space mode transition and stable storage motion can be realized in the designed field, as demonstrated by the calculation.

In practice, however, imperfections such as distortions of the magnetic field symmetry and deviations of the kicker current from the ideal waveform must be evaluated. This highlights the importance of accurately modeling the transient response of the kicker system.

The latter part of this paper focuses on the kicker coil geometry and the transient response of the pulsed current, and reports the current progress in evaluating the resulting distortions in the magnetic field distribution. Further details on the kicker current are given in Ref. [6].

KICKER

Figure 7 shows the kicker coil configuration together with a prototype model and its representation in the OPERA-3D simulation [7]. To evaluate the transient response of the pulsed current, the conductor must be modeled with an appropriate mesh size, particularly near the surface where

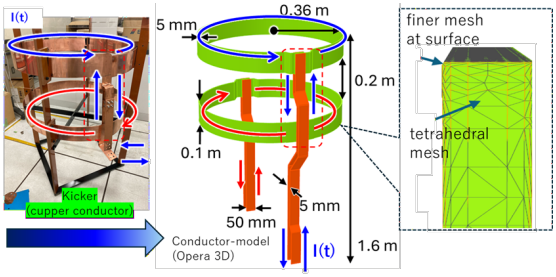

Figure 7: Kicker coil configuration, prototype, and OPERA-3D simulation model with surface-refined mesh.

the current distribution is strongly affected by the skin effect. Therefore, a refined tetrahedral mesh is applied in the near-surface region.

As the spatial field distribution is made closer to that of the actual device, the coil geometry becomes increasingly complex, requiring transient analysis based on the finite element method. In particular, transient simulations for a coil with a radius of 0.36 m driven by a fast pulse of 120 ns are not common, and the validation of the calculation itself becomes an important issue. In this study, a kicker coil model including the current input and output paths is constructed, and the reliability of the calculated magnetic field and its impact on beam injection are evaluated.

Transient Study for Skin Depth

The transient current distribution is governed by the skin effect, where the current decays exponentially from the conductor surface as $I(R)=I_0 \exp(-R/\delta)$. The skin depth is estimated to be about 32 μm for a pulse width of 120 ns (~4 MHz). The transient response on the conductor surface is evaluated using a tetrahedral mesh model.

Figure 8 compares the OPERA-3D simulation results of the kicker coil for slow (120 ms) and fast (120 ns) currents. In the 120 ns case, the skin effect causes the current to concentrate at the conductor surface, whereas in the 120 ms case the current is distributed throughout the conductor volume. This difference in current distribution leads to a clear change in the magnetic field profile at a given location as shown in Fig. 9. Therefore, the spatial distribution of the kicker field is strongly governed by the transient current distribution in the conductor.

Progress on Mesh Study

To reproduce the skin depth of 32 μm directly, the mesh size would need to be as small as about 10 μm (~ $\delta/3$). Such a straightforward treatment would require impractically large computational resources, with an estimated memory of 2.5×10^9 GB and a computation time of 1.7×10^{10} min. Therefore, a practical mesh strategy is required to calculate a physically reliable magnetic field distribution with limited machine resources. In this study, three mesh models are examined. To reproduce the skin effect efficiently, a layered mesh structure is adopted, with the outermost layer thickness set to 750 μm, 150 μm, and 32 μm (ver. 1-3), respectively.

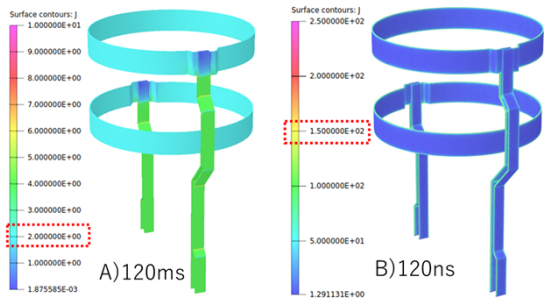

Figure 8: Comparison of current distribution in the conductor for slow (120 ms) and fast (120 ns) pulses.

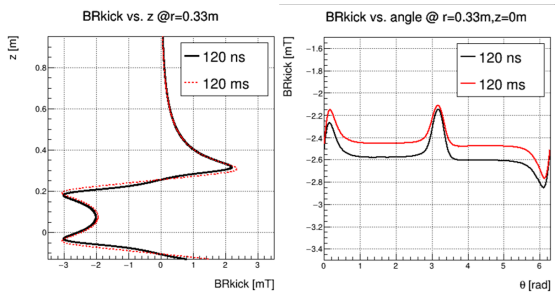

Figure 9: Magnetic field distributions showing differences induced by transient current effects.

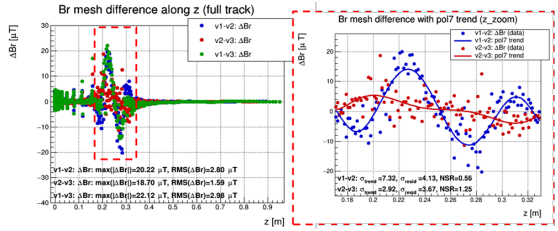

Figure 10: Magnetic field differences among mesh models demonstrating convergence of the calculation.

Figure 10 compares the magnetic field differences obtained with three mesh models (ver. 1-3). The horizontal axis represents the position along the solenoid axis, and the vertical axis shows the deviation in the calculated magnetic field. While differences are observed among the mesh models, the discrepancy between ver. 2 and ver. 3 is relatively small. This indicates that, for the present configuration, resolving the mesh down to the full skin depth is not strictly necessary for accurate magnetic field evaluation.

CONCLUSION

In this study, we demonstrated that the beam dynamics in the designed magnetic field can be well controlled through an appropriate injection scheme, and that the transient response of the kicker system plays a key role in determining the magnetic field distribution.

The comparison of different mesh models shows that the magnetic field calculation converges without resolving the mesh down to the full skin depth, indicating that a practical and computationally efficient modeling approach is feasible.

However, this result is based on an initial study, and further investigation is required.

REFERENCES

[1] H. Iinuma *et al*., "Three-dimensional spiral injection scheme for the g2/EDM experiment at J-PARC", *Nucl. Instrum. Methods Phys. Res. A*, vol. 832, pp. 51–62, 2016. doi:10.1016/j.nima.2016.05.126

[2] M. Abe *et al*., "Magnetic design and method of a superconducting magnet for muon $g-2$/EDM precise measurements in a cylindrical volume with homogeneous magnetic field", *Nucl. Instrum. Methods Phys. Res. A*, vol. 890, pp. 5-1-63, 2018. doi:10.1016/j.nima.2018.01.026

[3] S. Oyama *et al*., "Evaluation of the magnetic field error due to manufacturing tolerance of superconducting magnet for the J-PARC muon $g-2$/EDM experiment," *IEEE Trans. Appl. Supercond.*, vol. 33, no. 5, art no. 4001005 (5 pages), Aug. 2023. doi:10.1109/TASC.2023.3241828.

[4] H. Iinuma *et al.*, "Trajectory design for passing through solenoid magnet fringe field and method for adjusting its strongly X-Y coupled phase space for three-dimensional spiral beam injection", in *Proc. IPAC'25*, Taipei, Taiwan, Jun. 2025, pp. 2020–2023. doi:10.18429/JACoW-IPAC2025-WEPM029

[5] H. Iinuma *et al.*, "Beamline design and diagnostics for strong x–y coupled beams using a rotating auadrupole", presented at the 17th Int. Particle Accel. Conf. (IPAC'26), Deauville, France, May 2026, paper THP5620, this conference.

[6] Y. Kawase *et al.*, "Evaluation and mitigation of residual magnetic field from the high-voltage pulse power supply for the beam kicker in the muon g-2/EDM experiment", presented at the 17th Int. Particle Accel. Conf. (IPAC'26), Deauville, France, May 2026, paper TUP7711, this conference.

[7] OPERA-3D, Electromagnetic Simulation Software, Dassault Systèmes SIMULIA, https://www.3ds.com/products/simulia/opera